

Calibration and Upgrades of the XMM vertical EUV/X test facility : FOCAL X

Jean-Philippe TOCK, Jean-Paul COLLETTE, Yvan STOCKMAN

CENTRE SPATIAL DE LIÈGE - UNIVERSITY OF LIÈGE

Av. du Pré-Aily, B-4031 Angleur (Belgium)

phone : + 32 4 3676668, fax : + 32 4 3675613, email : CSLULG@ulg.ac.be

ABSTRACT

The X-ray Multi-Mirror Mission is the second of the four cornerstone projects of the ESA long term Programme for Space Science. The payload comprises three co-aligned high throughput imaging telescopes called Mirror Modules. The "Centre Spatial de Liège" (CSL) is in charge of optical and environmental qualification test of each of these MMs. To perform optical tests, a vertical test facility (FOCAL X) has been developed by CSL.

An EUV channel providing a 800 mm diameter collimated beam is used. A trade-off leading to the selection of an Electron Cyclotron Resonance EUV source is presented. Impact of the coating on the microroughness of the EUV optics is assessed and its homogeneity across the optical surfaces is measured.

Another feature of the facility is an X-ray channel providing a $50 * 8 \text{ mm}^2$ collimated beam. It has been characterised for X-ray effective area measurement. It is the first time that an off-axis parabolic mirror is used for this purpose.

Keywords: Test Facility, EUV optics, X-ray, Effective area measurement, XMM

1. INTRODUCTION

1.1. X-ray Multi-Mirror Mission

The X-ray Multi-Mirror Mission (XMM) is the second cornerstone of the ESA Horizon 2000 Science Programme^[1,2,3]. The main scientific goal of XMM is to perform high throughput spectroscopy of cosmic X-ray sources over a broad energy range (0.1 keV to 10 keV).

The XMM satellite payload includes three co-aligned high throughput imaging telescopes called Mirror Module (MM). Each MM is made of 58 confocal nested Mirror Shells (MS). The main MM characteristics are given in table 1.

A MS looks like a nearly cylindrical mirror made of Nickel with its internal surface coated with high purity gold, the external side being bare Nickel. The first part is a parabola and the second one an hyperbola, constituting a Wolter I telescope. The main MS^[4,5] characteristics are given in table 2.

At the exit of two of the three MMs, reflection grating spectrometers will be positioned. In the focal plane, X-ray CCD cameras will be installed.

XMM will be launched in late 1999, providing high capabilities to X-ray astronomers, offering a unique combination for X-ray spectroscopic measurements.

TABLE 1 : MM characteristics

HEW (on-ground performance)	< 16.5" at 58.4 nm < 16" 0.1 - 3 keV < 22" at 8 keV
Effective collecting area	> 1475 cm ² at 1.5 keV > 580 cm ² at 8 keV
Focal length	7500 mm 5 mm
Field of view	15 arcmin
Weight	425 kg

TABLE 2 : MS characteristics

Number of MS per MM	58
Length	600 mm
Outer diameter (hyperbola exit)	from 306.236 mm to 699.992 mm
Inner diameter (parabola entrance)	from 294.108 mm to 672.277 mm
Theoretical reflectivity (double reflection)	from 88 % to 73 % at 1.5 keV from 75 % to 0 % at 8 keV
Weight	from 2.35 kg to 12.30 kg
Thickness	from 0.47 mm to 1.07 mm
Minimum packing distance	1 mm

1.2. Basics

In 1994, for XMM optical testing, the only relevant European facility was the horizontal PANTER facility at the Max-Planck Institut für Extraterrestrische Physik (MPE) in Neuried (München) : an X-ray source at 130 m distance is available to illuminate in a slightly divergent beam the full aperture of the XMM MS or MM. Tests in this facility are nevertheless suffering two drawbacks :

- * The first 100 mm of the shells are not correctly illuminated in this configuration (beams reaching this part of the mirrors are not focalised at the focus position). The solution is to use a source more distant than 130 m or better, a collimated beam.
- * Adverse gravity effects are present on the shell/spider assembly. These effects are minimised when the telescope optical axis is vertical.

The ideal solution would be to test the telescope vertically in full illumination with an X-ray collimated beam in the operating range (between 0.1 keV and 10 keV). Unfortunately, at that time, the technology to realise this optical system was not available and it was unrealistic to consider the possibility to develop an X-ray parallel beam of more than 700 mm diameter in the allocated time (about one year).

The selected solution in FOCAL X (Facility for Optical CALibration at Liège in X-ray) was to develop a channel with a full illumination capability but at a longer wavelength and to limit the X-ray testing to partial illumination beams. The "full illumination" channel consists of an EUV channel at 58.4 nm. EUV has been preferred to visible because, at this wavelength, diffraction effects are small, compared to the telescope image quality. Two X-ray smaller beams have been added : one pencil beam for reflectivity measurements and one X-ray collimated beam for X-ray effective area measurements and image quality analysis.

1.3. EUV concept validation

In order to check the feasibility of image quality measurements in the EUV spectral range, a test campaign was conducted on single mirror shells in a facility existing at CSL : FOCAL 2 (Facility for Optical CALibration at Liège with a diameter 2 m). After half a year of intensive testing, the feasibility was demonstrated. Images were acquired and the analysis showed good correlation with results obtained in X-ray at the MPE.

1.4. Vertical test facility : FOCAL X

After this demonstration, the design and manufacturing of a vertical test facility (FOCAL X)^[6,7,8,9] started in June 1994, including a new building with a class 10 000 cleanroom of 28*18*15 m³. The digging started beginning of July 1994 and the office and cleanroom building with all technical infrastructures were finished end of April 1995. The facility was declared ready to receive the XMM Qualification Model Mirror Module in February 96. The general layout of the facility is given in figure 1.

In short, the facility is an optical test facility composed of a main vacuum chamber and three annexed chambers (one EUV chamber and two X-ray chambers). The facility is about 30 m high. The main chamber is a 4.5 m diameter vacuum chamber with a height of 12.2 m and a volume of about 190 m³. Three optical channels are available, sharing some general

resources like pumping system, vacuum chamber, cleanroom facilities, mechanisms, optical benches, computer control and data handling systems, analysis tools, control room, ...

The facility is designed to accept single Mirror Shell integrated on a rigid interface or hanging on a suspension device, Mirror Modules or Mirror Assemblies (MM equipped with a grating).

The XMM Qualification Model Mirror Module testing in FOCAL X^[10] started in March 96. The CSL test flow chart is given in figure 2. Single MSs were tested in the facility between the MM tests. In the first half of 97, FM1 MM and FM2 MM were tested^[11,12].

FIGURE 1 : FOCAL X GENERAL LAYOUT



FIGURE 2 : XMM QUALIFICATION MODEL MIRROR MODULE TEST FLOW CHART



2. EUV CHANNEL

2.1. EUV channel description

The EUV channel is presented in figure 3.A. The purpose is to provide an EUV collimated beam to achieve a full illumination of the MM over a diameter larger than 700 mm.

FIGURE 3.A : EUV CHANNEL

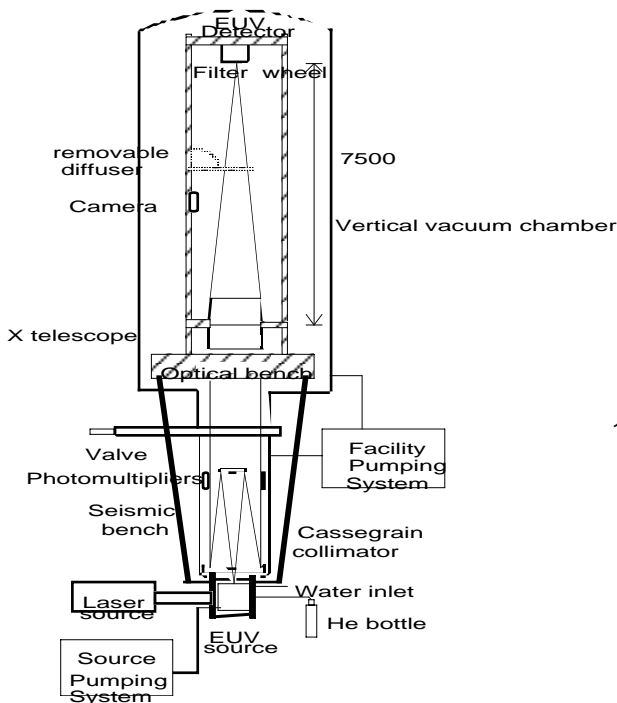
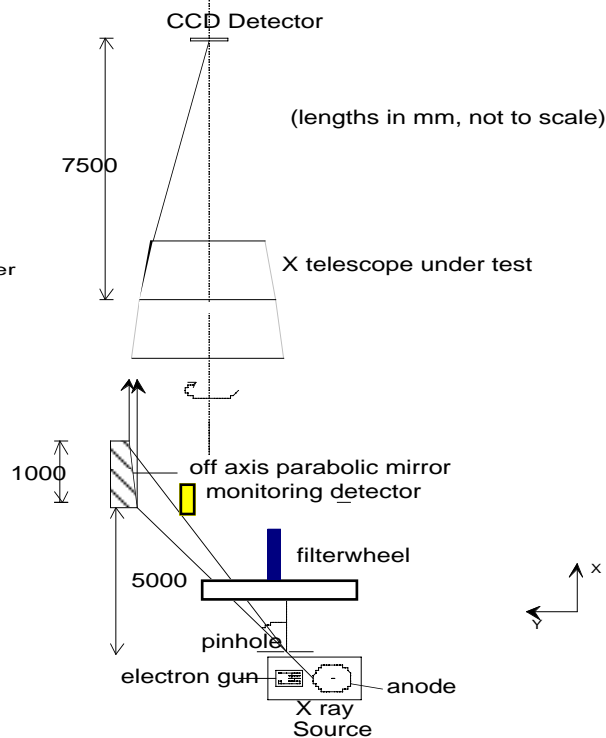


FIGURE 3.B : X-RAY COLLIMATED CHANNEL



2.1.1. The source

A trade-off has been carried out to select the most suitable source for this specific application. EUV sources are usually used in spectroscopy and surface science but less in characterisation of optical surfaces. A reliable device providing the maximum flux between 30 nm and 60 nm with a high luminance was required due to the amount of losses in the radiometric budget. Several types of sources based on different principles were available :

synchrotron radiation : it was the best choice for the available power but large investment and facilities, which were not compatible with our constraints, were required ;

XUV laser radiation : when we started the facility development, only prototypes were available and a sophisticated set-up was necessary to use such a source ;

Photoemission process : this type of source presented a too low luminance ;

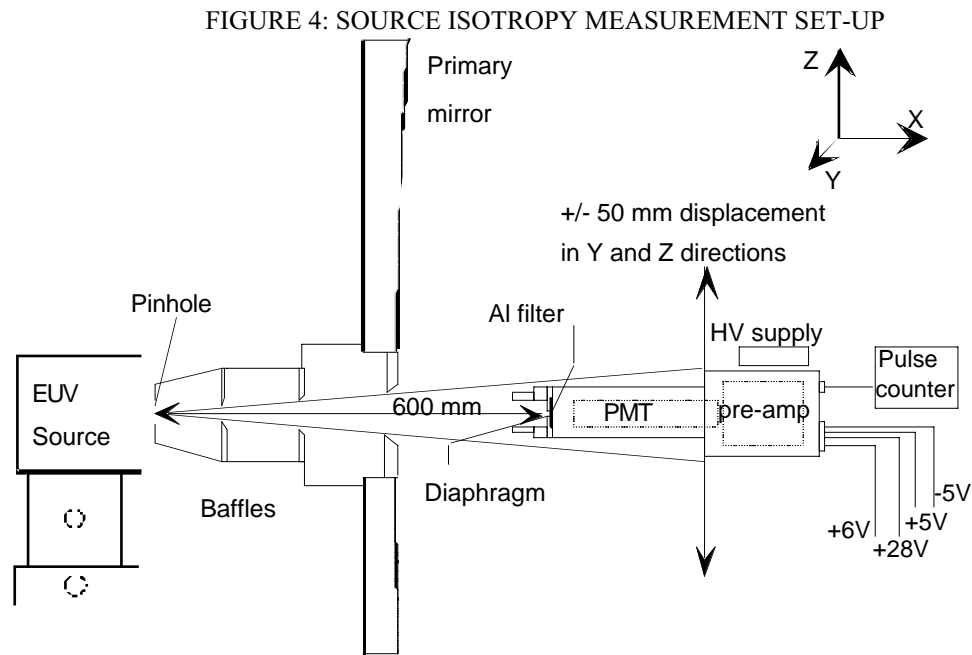
Open hollow cathode lamps : they were commercially available and usually relatively compact, stable and reliable.

Nevertheless, the selected EUV source was based on an Electron Cyclotron Resonance discharge, creating a light emitting plasma, claiming to be 10 times brighter than open hollow cathode lamps. For our application, the source is fed with

Helium, providing the He I line at 58.4 nm ($8 \cdot 10^{15}$ ph/sec*sr) and the He II line at 30.4 nm ($1 \cdot 10^{15}$ ph/sec*sr). A 100 μm pinhole, installed in front of the source emitting zone, is located at the focus of the collimator.

With open hollow cathode lamps, the emission isotropy is quite good thanks to their symmetrical design,. This characteristic was unknown in the case of the ECR source and should be experimentally evaluated. It had to be checked because the isotropy of the source would be replicated after two reflections on the collimator mirrors and so in the output beam. Experiments have been performed in another facility. The set-up is presented in figure 4.

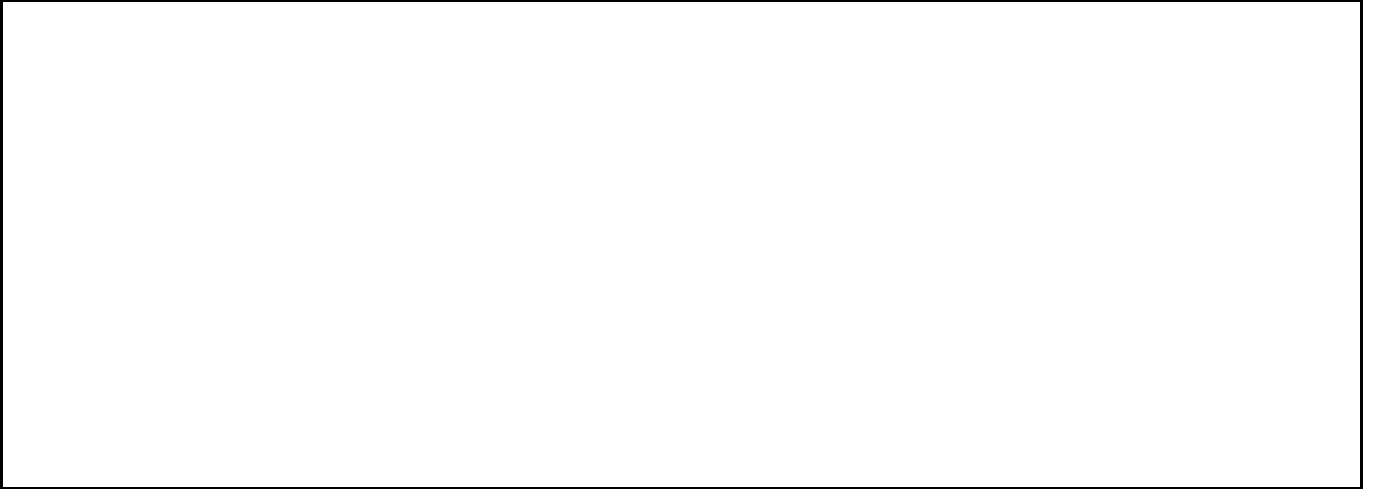
A Photo Multiplier Tube (PMT) detector was fixed on 2-D translation device at 600 mm from the source. This allowed to scan in a plane orthogonal to the source axis. The PMT is a 9826B Thorn EMI PMT, where a sodium salicylate coating is applied on the input window, in front of which a 1500 \AA thickness Al filter is fixed. It has been checked that this detector is only sensitive to EUV light. Two sources have been measured using this set-up : the selected ECR source and a hollow cathode source for comparison.



The results are presented in figure 5 which shows images of the cavity through the pinhole. The hollow cathode shows, as expected, good symmetry. The symmetry of the central core is consistent with the symmetrical design of the source. At first attempt, the ECR source presented a not centred intensity peak. The assumed reason was that the microwaves focusing point was not centred with respect to the mechanical parts. The source cavity was corrected and a new test was conducted.

After correction, the homogeneity of the ECR source was comparable to the one of the hollow cathode and satisfied the experiment needs. Moreover, the ECR source was about ten times brighter than the hollow cathode. Measurements performed in the collimator output beam^[7] have shown an homogeneity better than 10 %.

FIGURE 5 : EUV ECR SOURCE HOMOGENEITY BEFORE AND AFTER CAVITY CORRECTION



An additional visible source is also available. A He/Ne laser of 10 mW is used to provide a 633 nm beam. A pinhole, installed in front of the laser, is located at the conjugate focal point of the EUV collimator, by means of a removable folding mirror^[6]. The single MS alignment is possible to an accuracy of about 20 arcsec by using the hyperbola image shape. For integrated MM with 58 MS, the image at hyperbola focus is a mixture of 58 images coming from each single mirror and it is not possible to find an average "shape" or a useful qualitative criteria for alignment. One way should be to mask 57 MSs and to use the 58th as a reference. Since this procedure is quite complex, the procedure for MM is to co-align the EUV collimator optical axis with respect to the MM alignment lens. This alignment is checked under vacuum, using the maximum throughput as criteria.

2.1.2. The collimator

In front of the EUV and visible sources, a Cassegrain collimator provides a collimated beam of 800 mm diameter (internal obstruction : 250 mm diameter). The mirrors are both made of Zerodur, Platinum coated with a microroughness better than 10 Å. Figure 6 shows images taken at CSL with an optical profilometer. The same type of profilometer is also used to test the XMM MS micro-roughness^[4].

A particular care was taken in the microroughness specification. The objective was to get a scattering level lower than 5 %. The Total Integrated Scattering (TIS) is computed as follows^[13] :

$$TIS \approx \frac{4\pi}{\lambda} \cdot \delta^2 \quad (1)$$

where : TIS is the Total Integrated Scatter
 — is the RMS surface roughness
 — is the wavelength

To get a TIS lower than 5 % at 58.4 nm, the RMS surface roughness of the mirrors must be lower than 10 Å.

Tests were performed on the secondary mirror before coating. They were not performed on the primary mirror itself for handling and safety reasons but on its central drilled part, before and after coating. The central drilled part followed the same coating procedures as the mirrors themselves to be used as a witness sample. The secondary mirror microroughness is 8.2 Å, giving a TIS of 3 %. The primary mirror microroughness increased from 5.9 Å to 6.7 Å after coating, giving a TIS of 2 %, assuming that measurements on the central drilled part could be extended to the whole optical surface. The Peak-To-Valley variation is about 2 Å. On figure 7, the values obtained at various locations on the central drilled part of the primary mirror are shown. From the previous data, it can be seen that the polished and coated mirrors have an homogeneous surface as far as the microroughness is concerned.

FIGURE 6 : EUV COLLIMATOR MICROROUGHNESS MEASUREMENTS

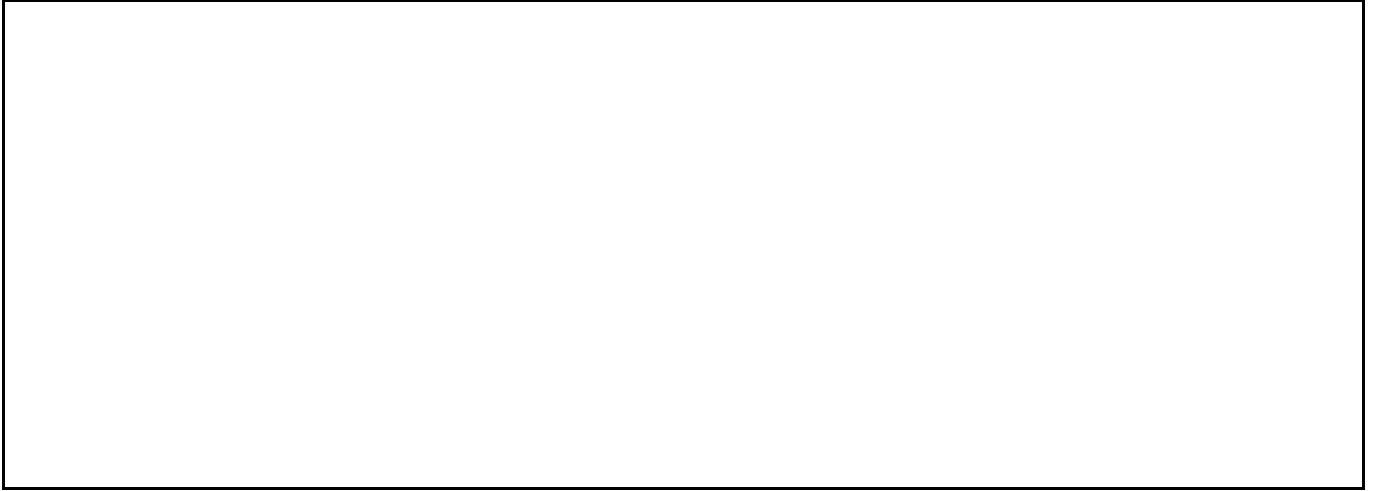
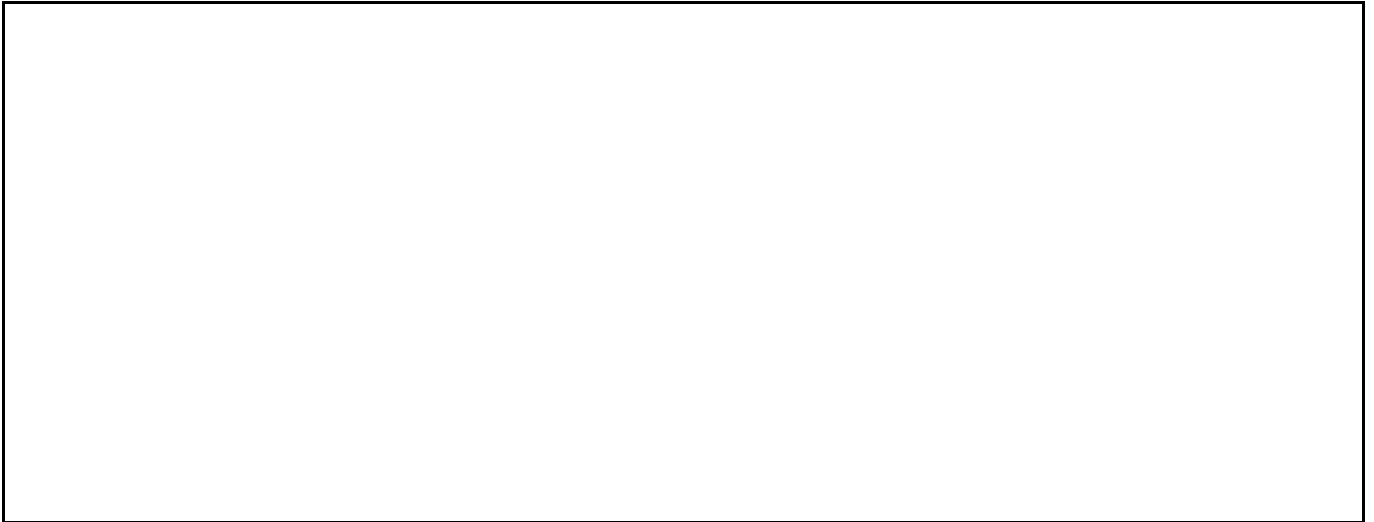


FIGURE 7 : MICROROUGHNESS MEASUREMENTS OF EUV COLLIMATOR PRIMARY MIRROR



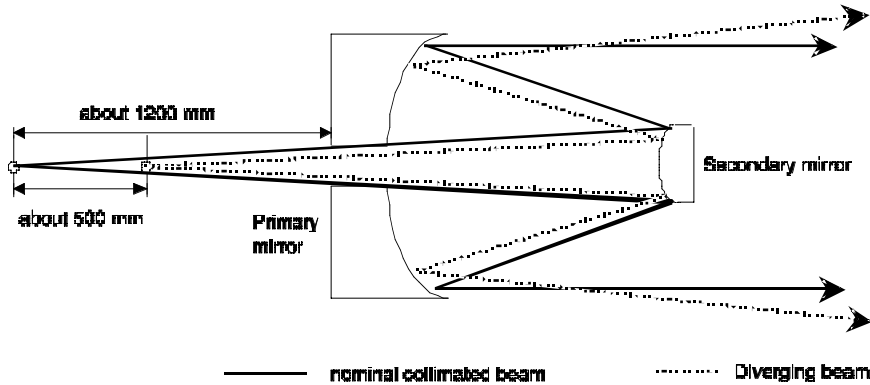
The coating was selected from theoretical reflectivity at normal incidence calculated from optical constant found in the literature^[14] and are given in table 3. Tungsten (W) would have been the best solution but was not possible taking into account schedule and geometrical aspects of our application. Platinum was finally selected for this collimator. The coating thickness was limited to 40 nm to avoid the risk to degrade the surface microroughness.

TABLE 3 : EUV REFLECTIVITY

<u>Metal</u>	<u>Reflectivity at 58.4 nm. [%]</u>	<u>Reflectivity at 30.4 nm. [%]</u>
Au	14.2	4.3
Ir	21.6	3.4
Pt	22	2.8
W	33	4.6

A problem arose with the comparison between data acquired at CSL with an infinite source distance and the results acquired at MPE with a source at 130 m. To be able to get and analyse comparable images, the collimator has been designed to have the capability to simulate a finite source distance. This is realised by moving the collimator pinhole and the EUV source towards the primary mirror. This required a long back-focal length as illustrated on figure 8. This capability is present but has not yet been tested.

FIGURE 8 : DE-FOCUSING PRINCIPLE



2.1.3. The photomultipliers

To check in situ the stability and the homogeneity of the collimated flux, four photomultipliers are installed in the collimated beam. They are working in the visible but the correlation between EUV and visible was checked by scanning the collimated beam with two detectors : one sensitive to visible only and one sensitive to EUV only.

2.1.4. The EUV detector

In the focal plane, an EUV thinned backside illuminated CCD is installed on a 3-axis translating mechanism. It has $1152 * 770 \text{ pixels}^2$ of $22.5 * 22.5 \mu\text{m}^2$. The working temperature of the CCD is -100°C . The detector is cooled via a liquid nitrogen cold plate and the temperature is regulated by heaters inside the camera. A filterwheel is installed in front of the detector. The different positions are given in table 4. Just before the filter-wheel, a shutter has been installed. Materials have been carefully selected and the cooling has been adapted to get a reliable system working under vacuum. The shutter is controlled manually or automatically by the EUV camera.

TABLE 4 : EUV CCD DETECTOR FILTERWHEEL

Position	Filter	Thickness [microns]	Diameter
1	shutter	/	/
2	aluminium	0.200	8 mm meshfree
3	aluminium	0.150	40 mm with a mesh
4	hole	/	40 mm
5	aluminium	2 * 0.150	8 mm meshfree
6	Al-carbon	0.150 (Al) +0.200 (C)	8 mm meshfree

TABLE 5 : X-RAY SOURCE TARGETS

Target	Quantity	Element number	Energy [keV]
Aluminium	7	13	1.5
Copper	5	29	8.04 8.90
Gold	2	79	2.1
Molybdenum	2	42	2.29
Carbon	2	6	continuous

TABLE 6 : X-RAY FILTERWHEEL POSITIONS

Position [number]	Material	Thickness [microns]
1	Hole	/
2	Al + Cu	40 + 5
3	Cu	20
4	Cu	50
5	Cu	100
6	Al	6
7	Al	20
8	Al	50
9	Ni	5
10	Ni	20
11	Ni	50
12	Ni	100
13	Cu	500
14	Cu	500
15	Cu	500
16	Stainless steel	1000 (shutter)

3. THE X-RAY COLLIMATED CHANNEL

3.1. X-ray collimated beam description

This channel provides an X-ray collimated beam as large as reasonably possible ($8 * 50 \text{ mm}^2$) and allows effective area and imaging quality measurement. This channel is mainly divided in 3 parts (see figure 3.B) : a source package, optics and detectors. This papers deals only with X-ray effective area measurements but the channel capabilities can also be used for imaging quality test.

3.1.1. X-ray source

An X-ray source is installed at the bottom of the channel. The anode of the source is equipped with various targets remotely selectable. They are listed in table 5. The projected emitting zone of the source is a disc of about 1 mm diameter.

In front of the source, a 18-position filterwheel is installed in order to select the appropriate lines and intensities and to reject the visible flux from the source. The available filters are listed in table 6 but other ones could be implemented.

3.1.2. Optical system

In front of the X-ray source, a Zerodur gold coated off-axis parabolic mirror is aligned, providing a vertical X-ray collimated beam with the shape depicted in figure 9. Its characteristics are given in table 7. A $100 \mu\text{m}$ diameter pinhole is at the focus of the parabolic mirror and is located inside the source.

FIGURE 9 : X-RAY COLLIMATED BEAM SHAPE

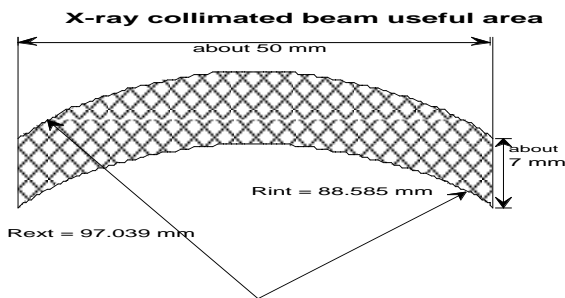


FIGURE 10 : X-RAY COLLIMATED BEAM MASK

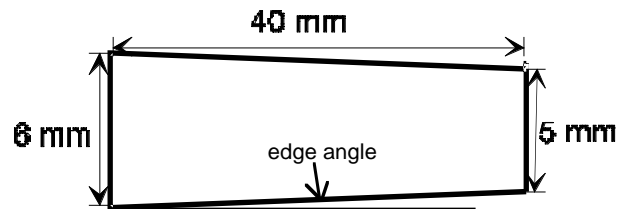


TABLE 7: OFF-AXIS MIRROR CHARACTERISTICS

<u>Optical useful area :</u>	length = 1000 mm. width = 50 mm.	
<u>Parabolic parameters</u>	$p = 0.784664 \text{ mm}$ $a = -0.392332 \text{ mm}$	$y^2 = 2 * p (x-a)$ with x,y Cartesian co-ordinates
<u>Microroughness</u>	0.137 nm RMS (frequency from 0.1 to 0.005 mm) 0.2 nm (frequency from 2 to 0.1 mm)	
<u>Coating</u>	gold ; 60 nm thickness	

3.1.3. Detectors

Three detectors are integrated in this channel. One monitoring detector and two in the focal plane.

In front of the parabolic mirror, in a non-used area, a solid state detector is installed to monitor the source intensity. Its characteristics are given in table 8.

Another solid state detector is installed on a 3-axis translation mechanism in the focal plane. Its characteristics are given in table 9. This detector having no spatial resolution, a slitwheel have been implemented in front of it. As the detector is on a translating device, it is possible to scan an image and to reconstruct it. On the same wheel, a shutter and a calibration source (Fe 55 giving lines at 5.9 keV and 6.4 keV) to calibrate and check the detector in situ are mounted.

TABLE 8 : SOLID STATE MONITORING DETECTOR

Crystal :	Silicium
Active surface :	7 mm ²
Energy resolution :	250 eV at 5.9 keV in situ
Window :	Beryllium 12.5 µm thick, meshfree
Operating temperature :	- 25°C
Cooling :	Peltier

TABLE 9 : SOLID STATE FOCAL PLANE DETECTOR

Crystal :	Germanium
Active surface :	500 mm ²
Energy resolution :	240 eV at 5.9 keV laboratory conditions
Window :	Beryllium, 20 mm diameter 13 µm thick, hexagonal mesh
Operating temperature :	- 150°C
Cooling :	Home-made dedicated liquid nitrogen cooling system

On the same 3-axis mechanism, close to the solid state detector, an X frontside illuminated CCD is installed. It has 1152 * 770 pixels² of 22.5 * 22.5 µm². Its working temperature is -100°C and is reached via a liquid nitrogen cold plate and heaters inside the camera itself.

The two X-ray focal plane detectors can be positioned in front of the two X-ray beams, using the upper optical bench translating tables.

3.2. X-ray effective area measurement procedure

Since the X-ray collimated beam has an aperture fairly smaller than the telescope entrance pupil, the procedure is to scan it by rotating and translating the telescope in front of the X-ray collimated beam. The incoming and outgoing fluxes are recorded and then compared to compute the X-ray effective area at the relevant wavelength.

3.2.1. Entrance flux measurement

The X-ray CCD detector is placed in the direct X-ray collimated beam and is operated in half frame transfer mode. A typical image obtained is given in figure 11. It can be seen that the flux is not perfectly homogeneous.

To minimise the error due to the inhomogeneity and the finite size of the beam, this one is positioned radially in front of the telescope entrance pupil. The best solution would be to have a well defined angular sector. For this reason a mask has been designed and manufactured. It will be aligned at the output of the collimator to limit the beam size to a known and practical shape. (see figure 10)

Ideally the edge angle should be adapted to each radial position. It was decided to take an optimum location, minimising the difference between the optimum angle and the actual one. The maximum relative difference is, for XMM, less than 3 %. This difference can be taken into account in the computation. The optimum edge angle is 0.7°.

The baffle length was fixed to 40 mm in order to cover the full telescope aperture in an entire number of turns. For XMM, five turns are necessary due to the difference between the outer and inner radius (200 mm).

To be strict, the two small sides of the baffle should be curved but they are straight. The error due to this approximation is less than 0.1 % and so is neglected.

Presently, this baffle is manufactured but not yet implemented. Anyway, by measuring the direct beam, it is possible to compute the exact section of the incoming flux. The flux is longer than the CCD and to cover the full beam, it is necessary to translate the detector.

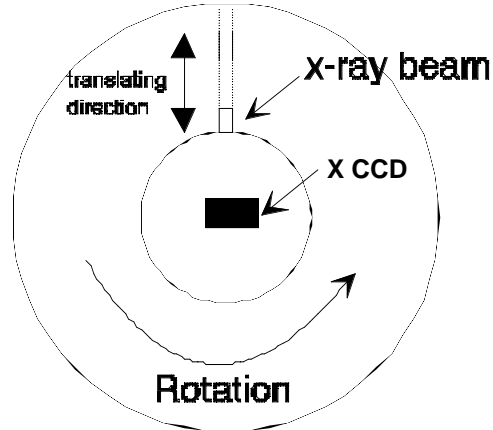
Due to the detector operating mode (half frame photons counting mode), it is necessary to check that there is no pile-up event and that the number of events is lower than 200 events per frame. If it is not the case, anode voltage or emission current can be reduced and/or a thicker filter could be positioned in the beam.

3.2.2. Under vacuum alignment

The next step is to move and to align the telescope in the X-ray beam. It is important to find the beginning of the innermost shell. The X CCD detector is moved on the optical axis at an extra-focal position of + 100 mm in order to decrease the number of pile-up events in the central core of the image.

FIGURE 11 : DIRECT FLUX IMAGE

FIGURE 12 : ALIGNMENT PRINCIPLE



During all this sequence, MM and detector are scanned synchronously, exactly the same way as a telescope and its detector rigidly linked. The MM is scanned in front of the beam until no more flux reaches the detector. The accuracy of this positioning method is better than 250 μm .

3.2.3. Reflected flux acquisition

When no flux is detected, a displacement corresponding to the cross section length of the collimated beam is performed to position the beam on the first ring of shells.

The specimen is then rotated by 360° and the flux reaching the detector is recorded during a full turn. Rotation mechanism has a stroke of 380° so the accelerating and decelerating parts of the motion are performed during the first and last 10° ; the full turn is therefore accomplished at a constant speed, adjustable between 5°/min to 72°/min.

A new flat field is acquired to check the stability of the system. Then a second ring is scanned by translating again the system of a distance equal to the collimated beam cross section length. This sequence is repeated until the full telescope entrance pupil is covered.

3.2.4. Results

At the end of the Flight Model 1 optical test campaign at CSL, opportunity was taken to test this procedure. For schedule reasons, only one intermediate ring was scanned and flat field acquired. It must be highlighted that the purpose of this experiment was to test and validate the measuring procedure more than characterize the telescope.

The procedure was applied with a rotation speed of 12°/min, giving a rotation time of 30 minutes. During a rotation, 130 frames are acquired, collecting about 20 000 events.

The applied formula is :

$$EA = \frac{\Phi_{out}}{\Phi_{in}} * F \quad (2)$$

where EA is the effective area, Φ_{out} the outgoing flux in ADU (Analog Digital Unit)/frame, Φ_{in} the incoming flux in ADU/(frame* cm^2) and F a correction factor taking into account the geometry of the set-up (collimated beam size, number of frames, ...).

For the ring scanned on FM1, a value of 357 cm^2 at 1.5 keV was obtained for a theoretical value of 363 cm^2 , that is a difference lower than 2 %.

3.2.5. Improvements

As already mentioned, a trapezoidal mask will be implemented to delimit accurately the beam and to have coverage of the entrance pupil corresponding to an entire number of turns.

The exposure times are presently measured by the manual opening/closure of a valve. To get a better knowledge of the exposure time, which is a key factor, a shutter synchronised with the acquisition time of the CCD camera, is under implementation.

At the time the measurements were performed, the source monitoring system (§4.1.3) was not available. Its integration in the data handling will give higher measurement accuracy.

Some software developments on partial events reconstruction would improve the procedure.

Use of other targets and filters will give effective area measurements at other wavelengths by using other spectral lines.

By using carbon target on the X-ray source giving a continuum spectrum and replacing the CCD detector by the solid state detector, it will be possible to measure in a single sequence, the X-ray effective area versus the incoming flux energy from about 1.5 keV to 17 keV. This procedure is under development.

4. CONCLUSIONS

The main features of FOCAL X, a facility dedicated to XMM, have been reminded. The EUV source isotropy has been demonstrated sufficient to perform valuable measurements, especially on XMM Mirror Modules. A procedure to measure X-ray effective area is also available.

The performance of the vertical test facility has been checked and shown in agreement with the required specification for the optical acceptance test of the XMM Flight Model Mirror Modules. Furthermore, new improvements are foreseen to increase the capabilities of a powerful test facility that could be used for the qualification of other X-ray telescopes.

ACKNOWLEDGEMENTS

The authors really wish to thank all their colleagues who worked very hard to develop the facility and to tune the facility operating procedures.

Many thanks go also to Dr H. Brauninger (Max-Planck Institut für Extraterrestrische Physik) and to D. Kampf (Kayser-Threde) for their help in the calibration and improvement process of the facility.

A special thank goes to Ph. Gondoin (ESTEC) for his precious help during the development and the application of the X-ray effective area measurement procedure.

The horizontal validation test has been supported by ESTEC under contract number 9939/92/NL/BS.

The vertical facility was funded by ESA XMM project under the ESTEC contract number 9939/92/NL/PP.

REFERENCES

1. D. Lumb, H. Eggel, R. Lainé, A. Peacock, "X-ray Multi-Mirror Mission - an overview", SPIE Denver 1996, Conference 2808-32
2. J. van Casteren, "The X-ray Multi-Mirror spacecraft, a large telescope", SPIE Denver 1996 conference 2808-33
3. Ph. Gondoin, D. de Chambure, K. van Katwijk, Ph. Kletzkine, D. Stramaccioni, B. Aschenbach, O. Citterio, R. Willingale, "The XMM Telescope", SPIE Vol 2279, pp86-100, 1994
4. D. de Chambure, R. Lainé, K. van Katwijk, J. van Casteren, P. Glaude, "The Status of the X-ray Mirror Production for the ESA XMM Spacecraft", SPIE Denver 1996, Conference 2808-35
5. D. de Chambure, R. Lainé, K. van Katwijk, J. van Casteren, P. Glaude, "The Status of the X-ray Mirror Production for the ESA XMM Spacecraft", SPIE San Diego 1997, Conference 3114-07
6. J.Ph. Tock, J.P. Collette, A. Cucchiaro, I. Domken, Y. Stockman, Ph. Kletzkine, A. Vignelles, "FOCAL X : a test facility for X-ray telescopes", 3rd International Symposium on Environmental Testing for Space Programmes, Noordwijk 1997.
7. J.P. Collette, Y. Stockman, J.Ph. Tock, Ph. Kletzkine, R. Lainé, A. Vignelles "Performance of XMM Optics vertical test facility", SPIE Denver 1996
8. A. Cucchiaro, I. Domken, P. Jamotton, I. Tychon and J.P. Tock "New facility for extreme ultraviolet and X-ray testing", 19th Space Simulation Conference NASA CP3341 Baltimore Octobre 1996
9. J.P. Collette, C. Jamar "X-ray and Extreme Ultra-Violet Test Facility of the XMM Optics", International Astronautical Federation, Oslo 1995
10. Ph. Gondoin, B. Aschenbach, H. Brauninger, D. de Chambure, J.P. Collette, R. Eggert, K. van Katwijk, D. Lumb, A. Peacock, Y. Stockman, J.Ph. Tock, R. Willingale, "X-ray Performance of a Qualification Model of an XMM Mirror Module", SPIE Denver 1996
11. Y. Stockman, J.Ph. Tock, E. Mazy, D. de Chambure, Ph. Gondoin "X-ray and EUV characterisation of the first XMM Flight Mirror Module", 3rd International Symposium on Environmental Testing for Space Programmes at ESTEC, Noordwijk, June 1997
12. Y. Stockman, J.P. Collette, J. Ph. Tock, D. de Chambure, Ph. Gondoin, "Optical testing of XMM Flight Module I and II at the vertical EUV/X facility", SPIE San Diego 1997, these proceeding
13. J.M. Bennet, L. Mattsson, "Introduction to Surface Roughness and Scattering", Optical Society of America, 1993
14. E.D. Palik, "Handbook of Optical Constants of Solids", Academic Press, 1985.